JOURNAL OF APPLIED PHYSICS VOLUME 93, NUMBER 7 1 APRIL 2003

Magnetic and magnetotransport properties of solid phase epitaxially grown Si:Ce films

T. Yokota, N. Fujimura,[a] and T. Ito
Graduate School of Engineering, Osaka Prefecture University, 1-1 Gakuen-cho, Sakai, Osaka 599-8531, Japan

(Received 5 June 2002; accepted 19 January 2003)

Magnetic and magnetotransport properties of a magnetic semiconductor, Si:Ce films, were investigated. The as-deposited films exhibit n-type conduction due to their amorphous nature, with a temperature dependence of the resistivity ($\rho - T$) like a normal semiconductor with diamagnetic properties. By annealing at 973 K, the conduction and the magnetic susceptibility change to the p-type and become positive, respectively. The change in the magnetic susceptibility ($\chi - T$) at a low magnetic field of 750 Oe against the measurement temperature exhibits spin-glasslike behavior showing a cusp around 38 K (T_g). The $\rho - T$ curve increases exponentially from 273 K to 35 K, and then drastically decreases by three orders of magnitude below 33 K. Above T_g, the magnetoresistance behavior at a magnetic field below 0.5 T can be understood as that of a semiconductor caused by the Lorentz force. Below T_g, on the other hand, an extremely large magnetoresistance, which can not be explained by a Lorentz force alone, is observed. © *2003 American Institute of Physics.* [DOI: 10.1063/1.1559436]

I. INTRODUCTION

Semiconductors doped with a magnetic element [diluted magnetic semiconductors (DMS)] have been widely studied, especially for the III–V (e.g., Mn-doped GaAs) and the II–VI (e.g., Mn-doped CdTe, etc.) compound semiconductors.[1–3] We have also been interested in Si-based DMS, which is a promising material, especially for microelectronics applications. In Ce-doped Si bulk samples, various phenomena, such as antiferromagnetism, heavy fermion-type transport behavior, and ferromagnetic ordering have been observed.[4] These bulk samples, however, have a polycrystalline structure with second phases such as Ce_5Si_4 and CeSi at the grain boundary that makes the investigation of its real magnetic and electrical properties difficult. To overcome such a structural issue, Si:Ce films were prepared using a vacuum evaporation system with electron-beam (EB) guns. Since the depositions were performed at a relatively low temperature of 400 °C to achieve films with high Ce concentration, the as-deposited films were amorphous and showed a semiconductorlike $\rho - T$ behavior with the n-type conduction and a diamagnetic behavior. By annealing at 973 K, the conduction type changed to the p-type, and anomalies in $\chi - T$ and $\rho - T$ curves appeared.[5] Although the annealed films had epitaxial structure and no silicide precipitation was recognized, a large number of defects, such as stacking faults and microtwins, were introduced during the solid phase epitaxial growth.[6]

In the present article, the magnetic and the magnetotransport properties of solid phase epitaxially grown SiCe films were carefully examined. The structure-relevant phenomena are discussed.

[a]Electronic mail: fujim@ams.osakafu-u.ac.jp

II. EXPERIMENTAL PROCEDURE

The amorphous Si:Ce films were deposited on (100) Si substrates by a conventional vacuum evaporation system using two EB guns. Silicon (with a purity of 99.9999%) and cerium (99.99%) were coevaporated at a growth pressure of 2×10^{-7} Torr. The deposition rates of Si and Ce were individually measured using thickness monitors. The composition of the films was evaluated by Rutherford backscattering. The thickness of the films measured by an α-stepped was obtained as 1200 nm. Since the as-deposited films were amorphous in structure, annealing was performed in a vacuum of 1.0×10^{-7} Torr. Auger electron spectroscopy was used to detect the impurities. The structure of the films was evaluated by conventional x-ray diffraction [(XRD) Shimazu XD-3A], high power XRD (Rigaku: RINT-1500), four-crystal XRD (Philips X′ Pert-MRD), and transmission electron microscopy [(TEM) JOEL-JEM-2000FXII]; we also investigated using transmission electron diffraction (TED). The magnetic properties were evaluated using a superconducting quantum interference device. The resistivity and the Hall effect were measured using the Van der Pauw method at temperatures ranging from 2 to 300 K. The magnetoresistance (MR) was replotted from current–voltage ($I - V$) measurements using a two-probe configuration at the elevated applied magnetic field at field up to 5 T.

III. RESULTS AND DISCUSSION

Si films having a Ce concentration ranging from 0.03 to 0.3 at. % were prepared at a deposition temperature of 400 °C. Although all samples behaved similarly in the magnetic and the magnetotransport properties, anomalies in these properties were most obvious in Si:0.3 at. % Ce films. Therefore, this article focuses on films at a Ce concentration of 0.3 at. %. The as-deposited film showed n-type conduction due

 © 2003 American Institute of Physics

Downloaded 25 Aug 2010 to 133.68.192.95. Redistribution subject to AIP license or copyright; see http://jap.aip.org/about/rights_and_permissions

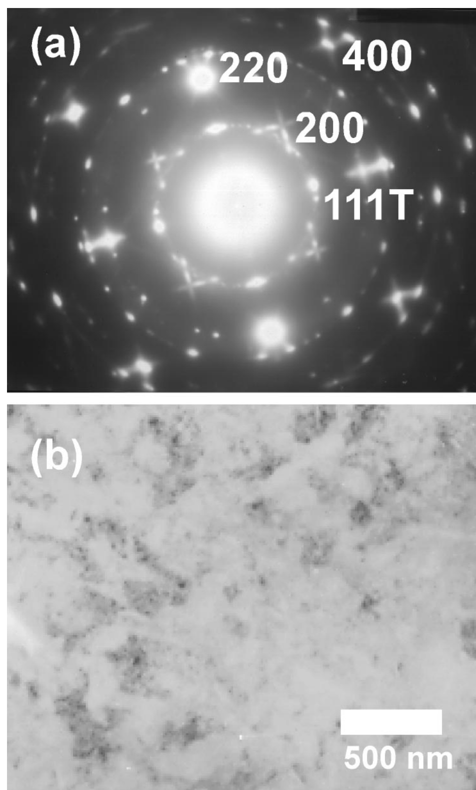

FIG. 1. TED pattern, (a) and the bright-field images of TEM, (b) from the solid-state epitaxially grown Si: 0.3 at. % Ce.

to its amorphous nature. A normal semiconductorlike $\rho-T$ behavior was observed. Diamagnetism due to the existence of the amorphous Si film and the Si substrate was recognized. In order to crystallize the film, the sample was annealed in the temperature range of 773 to 1273 K in a vacuum of 1×10^{-7} Torr. By annealing above 873 K, we confirmed solid phase epitaxial growth with expanded lattice constant using XRD and TED. The sample annealed at the 973 K for 10 h had the highest carrier density and magnetization. No silicide formation such as $CeSi_x$ (Refs. 7–9) was recognized even by detailed analysis of TED in the sample annealed below 1273 K. Figures 1(a) and 1(b) show the TEM and TED from the Si:0.3 at. % Ce annealed at 973 K

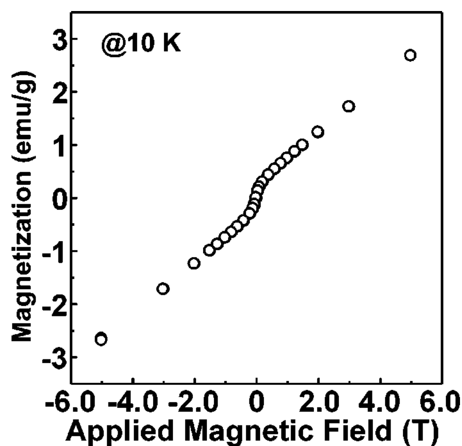

FIG. 2. Magnetization curve of epitaxial Si: 0.3 at. % Ce measured at 10 K.

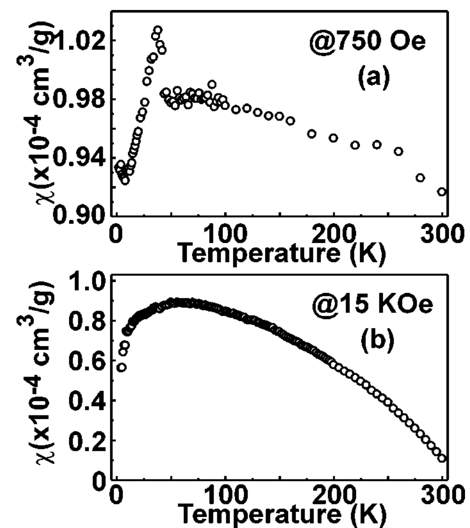

FIG. 3. Temperature dependence of magnetic susceptibility measured at the magnetic field of 750 Oe (a) and 15 kOe (b), respectively.

for 10 h, respectively. All the diffraction spots in the TED patterns were identified as being due to Si, and there are streaks through each of the 400 and 200 Si reciprocal lattice points due to the existence of stacking faults. The extra spots from microtwins were also observed. The dark regions widely dispersed in the sample with a diameter of around 10 nm were observed in TEM. The dark-field image of TED reveals that the dark regions observed in TEM correspond to the defects dispersed in the sample. TED, TEM, and XRD studies suggest that the epitaxially grown Si:Ce film contains widely dispersed defected regions (dark regions in TEM) with a higher Ce concentration probably due to the preferential dissolution of Ce to the defected regions. Since no silicide formation such as $CeSi_x$ has been recognized even by XRD and TED analyses, the defected regions were considered to be Ce-doped Si with a high Ce concentration.

Figure 2 shows the $M-H$ curve of the Si:0.3 at. % Ce film annealed at 973 K. The measurement was performed at 10 K. The magnetization curve has a steep slope below 0.1 T. This superparamagneticlike behavior[10] can be observed at least up to 300 K. These results indicate the existence of dispersed defected regions with a composition different from that of the matrix. Since the silicide precipitation and other ferromagnetic precipitation were not confirmed by detailed analyses by TEM, TED, and AES, each dispersed defected region containing a larger amount of Ce is assumed to have ferromagnetic coupling leading to superparamagnetic behavior. Since the $M-H$ curve at the magnetic field above 0.1 T shows linear magnetization behavior, the sample has not only a superparamagnetic component but also a paramagnetic component. Therefore, we performed $\chi-T$ measurements with low (750 Oe) and high (1.5 kOe) magnetic fields. Figure 3(a) shows the $\chi-T$ behavior measured at 750 Oe that should correspond to the magnetic behavior of the superparamagnetic component. The $\chi-T$ curve has a cusp at around 38 K. This magnetic property suggests that a spin-glasslike interaction[11] occurs among the defected regions. As the applied magnetic field increases, the shape of the cusp in the

Downloaded 25 Aug 2010 to 133.68.192.95. Redistribution subject to AIP license or copyright; see http://jap.aip.org/about/rights_and_permissions

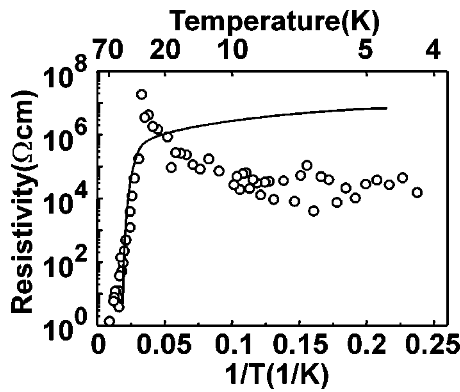

FIG. 4. Temperature dependence of resistivity; Solid line corresponds to the theoretical change of resistivity of the semiconductor calculated with the ionized impurity scattering and acoustic phonon scattering.

$\chi-T$ curve becomes smaller and broader. Figure 3(b) shows the $\chi-T$ curve measured at the magnetic field of 15 kOe. This $\chi-T$ behavior against the applied magnetic field is identical to that observed in a spin glass.[12]

Figure 4 shows the resistivity change against the inverse temperature. The solid line shows the theoretically calculated resistivity using ionized impurity and acoustic phonon scattering in a doped semiconductor.[13] The experimentally measured resistivity exponentially increases until 35 K with decreasing temperature and then it decreases by three orders of magnitude followed by an abrupt increase at the temperature between 35 and 33 K. Above 35 K, the resistivity change is well fitted by the calculated result. Below 35 K, however, the $\rho-T$ behavior cannot be explained only by the carrier scattering mechanism normally used for doped semiconductors because of the appearance of cusp in the $\rho-T$ behavior.

Considering the existence of the spin-frozen state, the $\rho-T$ behavior with a cusp becomes understandable. In the temperature range $T \gg T_g$, as the carrier transport occurs in the Si matrix with a smaller amount of Ce as compared with the defected regions, there should be little effect of spins dissolved in the Si matrix, which exhibit paramagnetism, on the carrier transport. The resistivity is also not affected by the spins at dispersed defected regions with a higher Ce concentration, which are responsible for the superparamagnetism. The field-cooled (5 T) $\rho-T$ curve at above T_g is identical to that without the external magnetic field, and it also supports the aforementioned speculation. At a temperature just above T_g, however, these defected regions begin to interact with each other and to affect the $\rho-T$ behavior. Below 35 K, therefore, the curve begins to deviate from the normal semiconductorlike behavior, and the resistivity abruptly increases after just a few degrees of temperature change, due to the magnetic fluctuation[14] among the defected regions with a ferromagnetic positive coupling. Each region then begins to make a frozen state (spin glass) just below T_g that is responsible for the drastic drop of the resistivity.

Judging from these speculations, since large MR is expected below T_g, we carefully investigated the temperature dependence of the MR at around T_g. Figures 5(a) and 5(b) show the MR curves measured at 70 K, which is higher than T_g, and at 30 K, which is almost the same temperature as

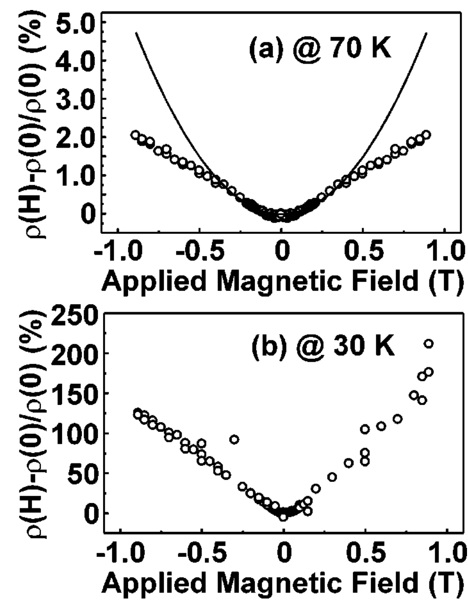

FIG. 5. MR measured at (a) 70 K and (b) 30 K. Solid line corresponds to the curve proportional to the square of the magnetic field.

T_g, respectively. The solid line in Fig. 5 corresponds to the fitting curve using a square dependence on the magnetic field. The magnetic field was applied perpendicular to the current direction. Both exhibit symmetric positive magnetization behavior. The MR measured at 70 K [Fig. 5(a)] shows quadratic behavior at a low magnetic field within 0.3 T that is normally observed in semiconductors with a low carrier density, and the Lorentz force is responsible for the positive MR.[15] This result is consistent with the $\rho-T$ behavior assuming that spins dissolved in the Si matrix are not consequential for the transport above T_g. With a decreasing measurement temperature, the magnetic field range in which the MR is proportional to the square of a magnetic field becomes lower. Approaching the T_g, the MR ratio becomes larger, probably due to the effect of spin fluctuations [Fig. 5(b)]. At a higher magnetic field, the positive MR seems to be suppressed by the effect of magnetic ordering in the Si matrix.

Below T_g, however, the MR behavior drastically changes. Figure 6 shows the MR measured at 10 K, which is

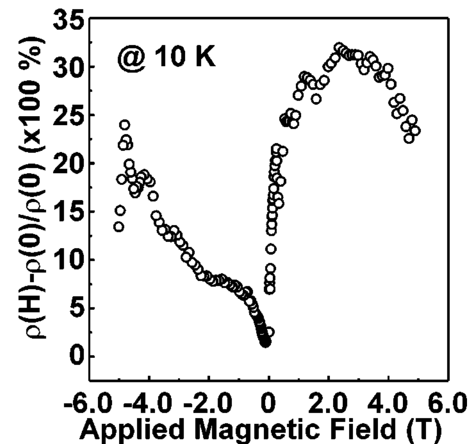

FIG. 6. MR measured at 10 K.

Downloaded 25 Aug 2010 to 133.68.192.95. Redistribution subject to AIP license or copyright; see http://jap.aip.org/about/rights_and_permissions

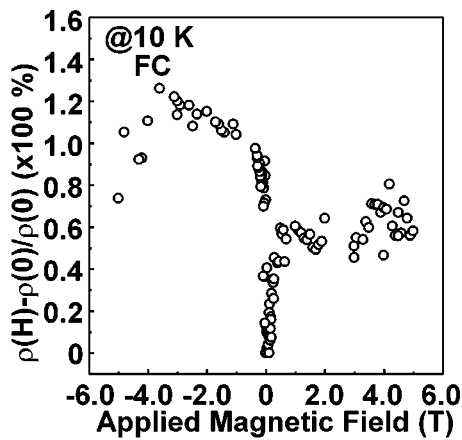

FIG. 7. MR field-cooled at 5 T measured at 10 K.

much lower than T_g. The measurement was performed at a magnetic field up to 5 T. A very large MR, exceeding 3000%, is recognized. The steep response of the resistance against the magnetic field within 0.5 T cannot be explained only by the effect of the Lorentz force. Below T_g, each defected region is in a frozen state with a random orientation. By applying the magnetic field, melting from the spin-frozen state takes place, which causes an increase in the resistivity by a spin–flip scattering process.[16] The MR curve, however, is neither linear nor symmetric. After applying a large positive magnetic field, some defected regions magnetically coalesce, thus causing an internal magnetic field in the sample. Once the internal magnetic field had taken place, the MR ratio decreased compared to that observed in the first measurement. This spin-glass state, including the internal magnetic field, may be responsible for the asymmetry of MR.

Thus, to study the internal magnetic field effect, we performed field-cooled MR measurements. Figure 7 shows the MR curve measured at 10 K after field cooling at a magnetic field of 5 T [field-cooled-magnetoresistance (FC-MR)]. After lowering the measurement temperature to 10 K under the applied magnetic field at 5 T, the magnetic field was removed, and we performed $I-V$ measurements without the magnetic field. The $I-V$ measurement was repeated at an elevated magnetic field until 5 T. The symmetry of FC-MR is reversed compared with that of zero-field-cooled MR (ZFC-MR), as shown in Fig. 6. Furthermore, the MR ratio decreases compared with that of ZFC-MR. This FC-MR result supports our speculation that there exists a spin-frozen state including an internal magnetic field. The phenomena described in the present article are quite similar to the blocking phenomenon observed in nonmagnetic materials with dispersed ferromagnetic particles.[11] In the present case, however, precipitations such as ferromagnetic particles were not recognized. Therefore, the positive magnetic interaction in each defected region is considered to be due to its high Ce concentration. If the regions with a high Ce concentration were uniformly spread in the whole sample, a ferromagnetic Si:Ce may be obtained.

IV. CONCLUSIONS

Anomalous magnetotransport behavior of a solid phase epitaxially grown Si:0.3 at. % Ce film has been observed. The magnetic susceptibility against the measurement temperature at the low magnetic field (750 Oe) exhibits spin-glasslike behavior showing a cusp at around 38 K. The temperature dependence of resistivity of the film also has a cusp at 33 K. The cusp in the $\rho-T$ curve originates from the spin fluctuations just above the spin-freezing temperature and following spin-glass formation. Below T_g, a very large MR which exceeds 3000% is recognized. The defected regions with a high Ce concentration are responsible for these magnetic and magnetotransport properties.

ACKNOWLEDGMENTS

This work was supported by a Grant-in-Aid for Scientific Research on Priority Areas (A), Spin Controlled Semiconductor Nanostructures (No. 10138218) from the Ministry of Education, Science, Sports, and Culture; a Grant-in-Aid for Scientific Research, No. 13875009; a Grant-in-Aid Exploratory Research, No. 13875009; a Grant-in-Aid for Scientific Research (S), No.14102021; a Grant-in-Aid for JSPS Fellows, No. 00000652, from the Japan Society for the Promotion of Science; and The Murata Science Foundation.

[1] H. Munekata, H. Ohon, S. von Molnar, A. Segmuller, L. L. Chang, and L. Esaki, Phys. Rev. Lett. **63**, 1849 (1989).
[2] S. von Molnar, H. Munekata, H. Ohno, and L. L. Chang, J. Magn. Magn. Mater. **93**, 356 (1991).
[3] S. Geschwind, A. T. Ogielski, G. Devlin, and J. Hegarty, J. Appl. Phys. **63**, 3291 (1988).
[4] N. Fujimura, Y. Morinaga, T. Yokota, and T. Ito, *Extended Abstract, The 4th Symposium on the Physics and Application of Spin-related Phenomena in Semiconductors* (Tohoku University, Sendai, Japan, 1998), pp. 105–108.
[5] T. Yokota, N. Fujimura, and T. Ito, Appl. Phys. Lett. **81**, 4023 (2002).
[6] T. Yokota, N. Fujimura, Y. Morinaga, and T. Ito, Physica E (Amsterdam) **10**, 237 (2001).
[7] S. A. Shaheen and J. S. Schilling, Phys. Rev. B **35**, 6880 (1987).
[8] S. A. Shaheen, J. Appl. Phys. **63**, 3411 (1988).
[9] S. A. Shaheen and W. A. Mendoza, Phys. Rev. B **60**, 9501 (1999).
[10] J. R. Childress and C. L. Chien, Phys. Rev. B **43**, 8089 (1991).
[11] K. Binder and A. P. Young, Rev. Mod. Phys. **58**, 801 (1986).
[12] P. J. Ford and J. A. Mydosh, Phys. Rev. B **14**, 2057 (1979).
[13] K. Seeger, *Semiconductor Physics*, 6th ed. (Springer, Berlin, 1996), pp. 161–225.
[14] T. Dietl, *Semimagnetic Semiconductors and Diluted Magnetic Semiconductors*, edited by M. Averous and M. Balkanski (Plenum, New York, 1991), 83.
[15] E. H. Putley, *The Hall Effect and Semiconductor Physics* (Dover, New York, 1960), p. 25.
[16] M.-T. Béal-Monod and R. A. Weiner, Phys. Rev. **170**, 552 (1968).

Downloaded 25 Aug 2010 to 133.68.192.95. Redistribution subject to AIP license or copyright; see http://jap.aip.org/about/rights_and_permissions